

# Deep learning-based fully automatic segmentation of wrist cartilage in MR images

---

Ekaterina Brui<sup>1</sup>, Aleksandr Y. Efimtcev<sup>1,2</sup>, Vladimir A. Fokin<sup>1,2</sup>, Remi Fernandez<sup>3</sup>, Anatoliy G. Levchuk<sup>2</sup>, Augustin C. Ogier<sup>4</sup>, Irina V. Melchakova<sup>1</sup>, David Bendahan<sup>4</sup>, Anna Andreychenko<sup>1</sup>.

<sup>1</sup> University of Information Technology Mechanics and Optics, International Research Center Nanophotonics and Metamaterials, 199034 S.-Petersburg, Russia

<sup>2</sup> Federal Almazov North-West Medical Research Center, 197341 S.-Petersburg, Russia

<sup>3</sup> APHM, Service de Radiologie, Hôpital de la Conception, Marseille, France

<sup>4</sup> Aix-Marseille Université, CNRS, Centre de Résonance Magnétique Biologique et Médicale, UMR 7339, Marseille, France

## **Corresponding Author contact information**

Ekaterina Brui,

e-mail: e.brui@metalab.ifmo.ru, katya.brui@gmail.com

tel: +7 9618112918

address: 199034, Russia, Saint Petersburg, Birjevaja line V.O., 14

## **ABSTRACT**

The objective of this study is to develop, test and validate a fully automatic, deep learning-based segmentation method for the wrist joint cartilage in magnetic resonance images. The study was conducted in 8 healthy volunteers and 3 patients with wrist joint diseases. 3D MRI datasets (20 in total) were acquired at 1.5T using a VIBE sequence. Wrist cartilage was segmented on coronal slices by a clinician and the convolutional neural network (CNN) was trained, developed and tested using the corresponding segmented masks. For an inter and intra observer study wrist cartilage was segmented by three observers once and twice by one observer on a dataset of 20 central coronal slices. Performance of the CNN was compared quantitatively to the manual segmentations using the concordance and the Sørensen–Dice similarity coefficients (DSC). Cartilage segmentations obtained with the CNN showed a substantial agreement with the manual segmentations for the whole wrist joint (DSC = 0.73) and a good agreement (DSC = 0.81) for the central coronal slices. The inter- and intra-observer concordance indices for manual segmentations were 0.55 and 0.85, respectively. The concordance index of the CNN-based segmentation was 0.69 when compared to the manual segmentations. The fully automatic deep-learning based segmentation of the wrist cartilage showed a high concordance with the manual measurements. It could be applied to determine an automatic, quantitative metric in clinical wrist cartilage studies.

## **ABBREVIATIONS USED**

CNN - convolutional neural network; DSC - Sørensen–Dice similarity coefficient; OA – osteoarthritis; RA - rheumatoid arthritis; RAMRIS - Rheumatoid Arthritis Magnetic Resonance Imaging scoring; JSN - joint space narrowing; GT - ground truth; CI - concordance index.

## **INTRODUCTION**

Magnetic resonance imaging (MRI) of joints has been recognized as a promising valuable tool for the diagnosis of osteoarthritis (OA) and rheumatoid arthritis (RA)<sup>1,2</sup>. One of the possible quantitative biomarkers for these diseases is the cartilage volume. While conventional X-Ray method estimates cartilage degradation indirectly through the joint space narrowing (JSN)<sup>3</sup> MR images display a superior soft tissue contrast that could be used for a straightforward assessment of the cartilage volume<sup>4,5</sup>. This illustrates that MRI is a promising alternative diagnostic tool for the detection of early cartilage changes in degenerative diseases of joints<sup>4</sup>. Measurements of the JSN from MR images have been proposed to be added to the RAMRIS (Rheumatoid Arthritis Magnetic Resonance Imaging scoring) system in order to include the cartilage loss assessment in the diagnosis of RA<sup>6</sup>. However, this cartilage loss scoring methodology demands manual measurements of the cartilage thickness on a carefully preselected slice between all articulation surfaces of a joint. For a knee joint, it implies four manual measurements whereas for a wrist joint it results in fifteen measurements, due to the complex structure of the wrist joint as compared to the knee. In addition, this assessment only provides a rough estimation of the cartilage changes at fixed points and therefore lacks sensitivity for the detection of the early subtle degradations. In OA diagnostics, recent studies show that longitudinal change in cartilage thickness measured with MRI is a more reliable quantitative metric for cartilage assessment than JSN measured from conventional X-ray<sup>7</sup>.

Several alternative criteria such as a cartilage cross-sectional area and cartilage volume have been proposed for the evaluation of cartilage loss in joints<sup>8,9,10</sup>. Measurement of the corresponding parameters requires a careful selection and segmentation of cartilage voxels on MR images, which

is challenged by the presence of other tissues such as synovial fluid or edema areas that often display a similar MR contrast. Several types of cartilage segmentation methods have been proposed in the literature. Segmentation has been performed manually with or without a dedicated radiological software<sup>9,11,12,13</sup> and combined with a thresholding procedure<sup>8,14</sup>. A wide range of computer-assisted approaches has been proposed: semi-automated procedures based on radial intensity profiles<sup>15</sup> or bespoke approach<sup>16</sup>; and fully automatic segmentation procedures<sup>17,18,19,20</sup>. The manual methods are commonly considered as the most reliable although they are recognized as highly time consuming. More recent semi-automatic and fully automatic technologies have been able to segment cartilage significantly faster with only a moderate penalty regarding accuracy. Considering the manual segmentation as the ground-truth, semi-automatic and fully automatic methods have been characterized by Sørensen–Dice similarity coefficient (DSC) up to 0.88<sup>15,16</sup> and 0.80<sup>17</sup>, respectively. More recently, promising results have been obtained using a convolutional neural network (CNN) developed for the fully automatic segmentation of knee MR images<sup>21,22,23,24</sup>. The corresponding DSC values were around 0.82 for the tibial<sup>21</sup> and around 0.80 for the cartilage of different knee joint surfaces<sup>24</sup>.

While most of the above mentioned methods have been dedicated to knee MR images, very few methods<sup>8,10</sup> have been developed for wrist MR images most likely due to the wrist joint anatomy complexity. Considering this complexity, manual segmentation of wrist cartilage is recognized as a highly time-consuming and tedious method, and to the best of our knowledge, no automatic or semi-automatic procedures have been developed so far. Considering the outstanding performance of CNN for the segmentation of the knee structures, we hypothesized that a dedicated CNN could perform as well for the fully automatic segmentation of wrist cartilage.

In the present study, a CNN was developed for the fully automatic segmentation of the wrist joint cartilage and compared to the manual segmentations performed by experienced radiologists.

## **PATIENTS AND METHODS**

Eight healthy volunteers with no previous wrist trauma (six males and two females, age range 23-38, mean 29.6) and three patients were included in the study after a written informed consent was obtained. Among the three patients, two suffered OA (female, 63 and 77 years old) and one was complaining about articular pain without the confirmed diagnosis (female, 62 years old). The study was approved by the local ethics committee. All data were acquired in a time period from 01/12/2017 to 01/05/2018.

### **MR-imaging**

MR images were acquired at 1.5T (Magnetom Espree Siemens) and subjects were asked to lie still in the so-called “superman” position (prone position with an outstretched arm, that is standard for wrist imaging). The wrist was imaged with a conventional birdcage type transmit/receive coil (CP Extremity Coil, Siemens Healthcare GmbH) and/or a home-made wireless coil that allowed to achieve higher signal-to noise ratio<sup>25</sup>. A total of 20 imaging sessions were held for all the 11 subjects. 3D coronal T1-weighted gradient echo (VIBE - Volumetric Interpolated Breath-hold Examination) images were acquired with fat suppression as previously described (Zink et al., 2015) in order to achieve an optimal contrast-to-noise ratio for the cartilage. The relevant parameters were: TR/TE = 18.6/7.3 ms, FoV = 97x120 mm<sup>2</sup>, matrix - 260x320, voxel size = 0.37x0.37x0.5 mm<sup>3</sup>, number of coronal slices = 88, flip angle = 10°, total acquisition time = 6 min.

## Data preparation

Each 3D dataset was subsequently converted into multiple 2D coronal images (1760 slices in total) (fig. 1(a)). Wrist cartilage was manually segmented<sup>8</sup> on 341 slices, among which 189 were used for the training phase of the CNN, 20 for the development phase, 112 for the test phase and 20 for the validation phase. Validation included a comparative analysis between the results of the developed neural network and those from a manual segmentation procedure performed by three observers. Datasets for the training, development and test stages contained only the data from the healthy volunteers. Images used for the test phase (images of cases #1 - #10) were not used for the training and development dataset (images of cases #10 - #15), i.e., the CNN was tested on the images of previously unseen subjects. The validation phase was performed for the slices of interest (medial slices) chosen from 3D wrist images for all 20 cases (both healthy volunteers and patients) on the basis of criteria similar to what has been previously described<sup>8</sup>. These slices were excluded from training, development and test datasets (i.e. slices unseen by CNN).

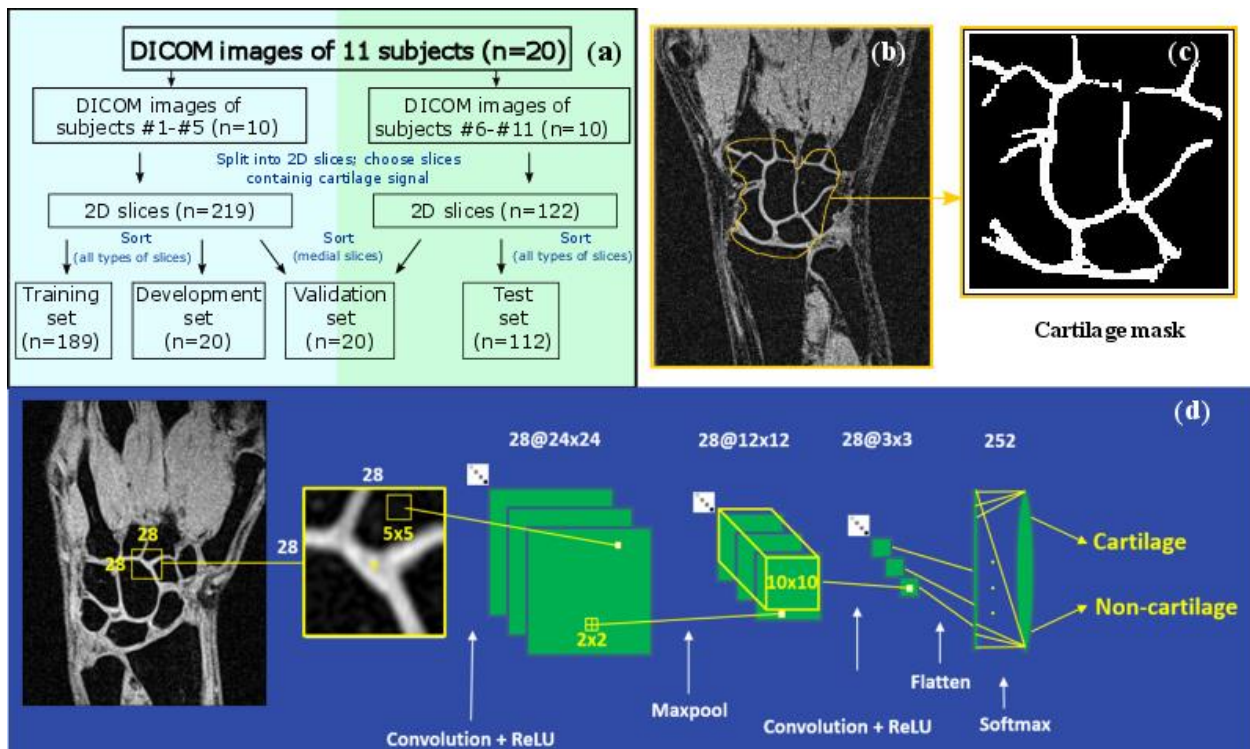


Figure 1. Schematic representation of data splitting for the different stages of the CNN development (a). Manual segmentation of the wrist cartilage (b). Final binary mask (c) obtained after thresholding and manual correction (c). Architecture of the developed CNN (d). DICOM - Digital Imaging and Communications in Medicine.

## Manual segmentation procedure

For the slices included in the training, development and test datasets, cartilage areas were manually segmented by an expert radiologist (O1 - V.F.). The wrist joint was initially roughly manually delineated for each slice (fig. 1(b)) and a thresholding procedure was performed using MATLAB (The MathWorks, Natick, Massachusetts). The resulting images (fig. 1(c)) were manually

corrected and the corresponding binary masks were used for the training, development and test phases.

### **CNN architecture**

Given that the wrist joint anatomy is significantly more complicated than the knee joint, we did not use an existing network but developed a genuine CNN architecture tailored for the wrist joint. During the development of the corresponding CNN architecture, multiple network parameters were investigated such as the number of layers, the input patch size, the number of features of the convolutional layers. As illustrated in figure 1d, the final CNN architecture had five layers and a two-class output. The network input was a 28x28 pixels patch surrounding the pixel to be classified. Training and testing sessions were performed using a computer with random access memory - DDR3 512Gb, central processing unit - Intel Xeon E5-4617 2.90 GHz (4 processors), and operating system - Windows Server 2012 R2 Standard 64-bit. The Python dynamic object-oriented programming language, version 3.6.4, TensorFlow and Keras open-source neural network library were used for building the CNN.

Cartilage masks manually segmented on each coronal slice of the training dataset resulted in a total of  $260 \cdot 10^3$  cartilage pixels out of  $13.8 \cdot 10^6$  pixels. As previously described<sup>22</sup>, for each pixel of interest, a 28x28 patch with this pixel at the center was used as a network input. The development dataset included  $1.5 \cdot 10^6$  pixels in total and  $24 \cdot 10^3$  pixels of cartilage. For each image, the network output was a probability map calculated on a pixel basis that was then thresholded to obtain cartilage binary masks. The threshold value was optimized within the development dataset. The resulting CNN was evaluated on the test dataset ( $8.2 \cdot 10^6$  pixels) and the obtained binary cartilage masks were compared to the manually segmented masks ( $182 \cdot 10^3$  pixels of cartilage) using DSC as a quantitative metric<sup>26</sup>:  $DSC = 2|X \cap Y| / (|X| + |Y|)$ , where X is a manually segmented binary mask and Y – segmented by CNN.

For the test dataset, DSC values were averaged over the total number of slices. Then they were compared with those from the previously developed CNNs for cartilage segmentation of the knee joint<sup>21,24</sup>.

### **Data analysis**

#### *Reproducibility of the manual segmentation procedure*

Manual segmentation of the wrist cartilage was performed on the validation dataset once by 2 experts (O2 - A.E., O3 - R.F) and twice (1 week between the segmentation sessions) by 1 (O1 – V.F.). All the 3 observers had 10 years experience in musculoskeletal segmentation. The manual segmentations performed by the observer O1 at the first session was considered as the ground truth (GT). Validation dataset included  $1.5 \cdot 10^6$  pixels in total and  $37 \cdot 10^3$  pixels of cartilage. The corresponding cartilage volume ( $V_{ijm}$ ), where i refers to the observer number (from 1 to 3), j to the session number (from 1 to 2) and m to the case number (from 1 to 20) was calculated as a product of the number of pixels within the resulted binary mask and the pixel volume ( $0.37 \times 0.37 \times 0.5 \text{ mm}^3$ ). For each observer, the averaged cartilage volumes were calculated. In order to determine the variability of the manual segmentation procedure, the concordance index (CI) was calculated. Case specific interobserver  $CI_m$  was measured subsequently between individual volumes,  $V_{ijm}$ , segmented by all observers in the first sessions:

$$CI_m^{inter} = \frac{V_{11m} \cap V_{21m} \cap V_{31m}}{V_{11m} \cup V_{21m} \cup V_{31m}}. \quad 1$$

Then the case specific interobserver CI was averaged over the total number of cases (M=20):

$$\overline{CI_m^{inter}} = \frac{\sum_m CI_m^{inter}}{M}, \quad 2$$

and its standard deviation was determined.

The intra-observer variability of the manual method (for segmentations repeated twice by O1) was also evaluated using the CI:

$$CI_m^{intra} = \frac{V_{11m} \cap V_{12m}}{V_{11m} \cup V_{12m}}, \quad 3$$

and was averaged over all cases in a same way as  $CI_m^{inter}$ .

### *Comparison of CNN-assisted and manual wrist cartilage segmentations*

The assessment of CNN performance was evaluated from a comparative analysis with the manual segmentation, i.e., binary cartilage masks were calculated from the network output and compared to the manually segmented masks. For each case, the volume of the segmented cartilage  $V_{m\_NN}$  and the GT volume,  $V_{m\_G}$ , were compared using CI (equals in this case to the Jaccard index<sup>27</sup>), and the resulted values were averaged over all cases:

$$\overline{CI_{m\_NN}} = \frac{\sum_m \frac{V_{m\_NN} \cap V_{m\_GT}}{V_{m\_NN} \cup V_{m\_GT}}}{M}, \quad 4$$

and the standard deviation was determined.

## **RESULTS**

### **Manual segmentation procedure**

The averaged cartilage volume determined by each observer was  $127.6 \pm 24.1 \text{ mm}^3$ ,  $125.7 \pm 20.8 \text{ mm}^3$  and  $130.5 \pm 19.1 \text{ mm}^3$  for O1, O2 and O3 respectively. Statistics for the manually performed segmentation procedure are summarized in Table 1. The consistency of manual segmentation procedure was evaluated using the interobserver CI, which reached  $0.55 \pm 0.07$  for the whole subject group;  $0.55 \pm 0.07$  for the healthy volunteers and  $0.55 \pm 0.05$  for the patients. An average time needed for an observer to segment manually all 20 slices was about one hour.

Table 1. Statistics for manual and CNN-assisted cartilage segmentation procedures.			
# of case	Intraobserver CI	Interobserver CI	CNN CI (Jaccard index)
1*	0.86	0.57	<b>0.79</b>
2*	0.85	0.65	<b>0.72</b>
3*	0.78	0.50	<b>0.71</b>
4*	0.72	0.49	<b>0.72</b>
5*	0.95	0.59	<b>0.75</b>
6*	0.88	0.59	<b>0.69</b>
7*	0.77	0.60	<b>0.61</b>
8*	0.81	0.58	<b>0.65</b>
9*	0.87	0.58	<b>0.64</b>
10*	0.88	0.50	<b>0.67</b>
11*	0.95	0.55	<b>0.72</b>
12*	0.96	0.54	<b>0.72</b>
13*	0.85	0.60	<b>0.70</b>
14*	0.85	0.35	<b>0.59</b>
15*	0.77	0.61	<b>0.68</b>
16**	0.76	0.59	<b>0.61</b>
17**	0.96	0.47	<b>0.56</b>
18**	0.77	0.58	<b>0.80</b>
19**	0.87	0.58	<b>0.59</b>
20**	0.92	0.52	<b>0.72</b>
Averaged over cases	0.85	0.55	<b>0.68</b>
SD	0.07	0.07	<b>0.07</b>
* - Healthy volunteers, ** - Patients. SD – Standard deviation, CI – concordance Index, CNN – convolutional neural network.			

### CNN segmentation

After the training session, the designed network was able to segment successfully cartilage pixels on VIBE MRI scans as illustrated in figure 2a. Red color corresponds to true positives, i.e. pixels correctly segmented as cartilage; green – to false negatives, i.e. pixels incorrectly assigned to a background; and blue – to false positives, i.e. pixels incorrectly assigned to cartilage. The mean DSC obtained for the test phase was  $0.73 \pm 0.11$ .

Statistics for the CNN-based cartilage segmentation procedure for the validation phase are presented in Table 1. The averaged CI relative to GT was  $0.68 \pm 0.07$ . The corresponding values for healthy volunteers and for patients were  $0.69 \pm 0.05$  and  $0.65 \pm 0.10$ , respectively. For the validation dataset, the averaged DSC was  $0.81 \pm 0.11$  and the averaged cartilage volume was  $134.8 \pm 20.9$  mm<sup>3</sup>. The duration of a typical segmentation procedure for 20 images was 5 minutes.

## DISCUSSION

The aim of the present study was to design and assess the performance of a genuine CNN for the wrist cartilage segmentation. While manual segmentations performed twice by the same observer showed a relatively high concordance, the between operators concordance was lower and ranged between 0.47 and 0.65 likely as a result of the wrist joint anatomy complexity combined with the fact that thresholds chosen by observers could have been different. Considering these values of CI, different observers agreed only for 65% of the segmented pixels.

For the CNN-assisted segmentation of the test set, a substantial agreement<sup>28</sup> was observed considering the manual segmentation as the ground truth. The corresponding DSC value (0.73) was slightly lower than for the previously reported CNN-assisted knee cartilage segmentation (0.80-0.82)<sup>21,24</sup>. However, this value can be considered as highly satisfactory given the significantly more complex anatomy of the wrist joint. Interestingly, the DSC value obtained for the validation set, i.e. 20 medial coronal slices, was larger (0.81). This could be explained by the fact that medial slices displayed a high contrast-to-noise ratio and a large amount of cartilage pixels whereas lateral (e.g., fig. 2(b)) slices included in the test set had a lower contrast-to-noise ratio. Overall, the developed CNN might be considered as optimal and ready to be used for the automatic calculation of cartilage cross-sectional area as previously suggested<sup>8</sup>.

The CI (0.68) of the CNN was lower as compared to the manual intra-observer result (0.85) whereas it was larger than the inter-observer result (0.55). One has to keep in mind that the same observer (O1) segmented the wrist cartilage for the training dataset and the intra-observer study. The lower CI value indicates that CNN did not fully reproduce the manual segmentation approach of observer 1. The detailed analysis of the cartilage masks provided by the CNN showed that a thin layer of subcutaneous fat was occasionally considered as a cartilage area by the CNN (circled areas on fig. 2(b,c,f)). However, when considering the inter-observer CI value, the CNN-based segmentation was better. In other words, the designed CNN provided reproducible results whereas the manual segmentation performed by different observers was largely heterogeneous indicating a low reproducibility.

Given the fact that the training dataset did only include healthy joints, we expected a lower CI for patients data during the validation stage. On the contrary, the results obtained for both manual and CNN assisted segmentation did show similar CIs for healthy volunteers and patients. Images of all patients, both with confirmed and not confirmed OA, contained pathological changes. The patient without the confirmed OA diagnosis had intraosseous ganglion cyst in the radial aspect of the triquetral and cortex erosions (fig. 2(d)). The first and the second patients with confirmed OA had intraosseous ganglion cysts in capitate (fig. 2(e)) and bone marrow edema in lunate (fig. 2(f)) bones, respectively. Although these structures could be misclassified as cartilage considering the signal intensity, these lesions were not classified as cartilage by the CNN. Interestingly, a vessel in a capitate bone of the second patient, having a structure and contrast extremely similar to the cartilage, was not segmented by CNN as well. These important results demonstrate the capability of the developed CNN to distinguish cartilage from both other anatomical structures and possible joint abnormalities.

We acknowledge several limitations in the present study. We used a training dataset from a small number of subjects and with a single manual segmentation. In order to improve the segmentation performance of the developed CNN further, more subjects and/or data augmentation methods could be used. In addition, multiple manual segmentations could be added to the training dataset



instead of a single one. As a future step, we plan to include more pathological images in the training

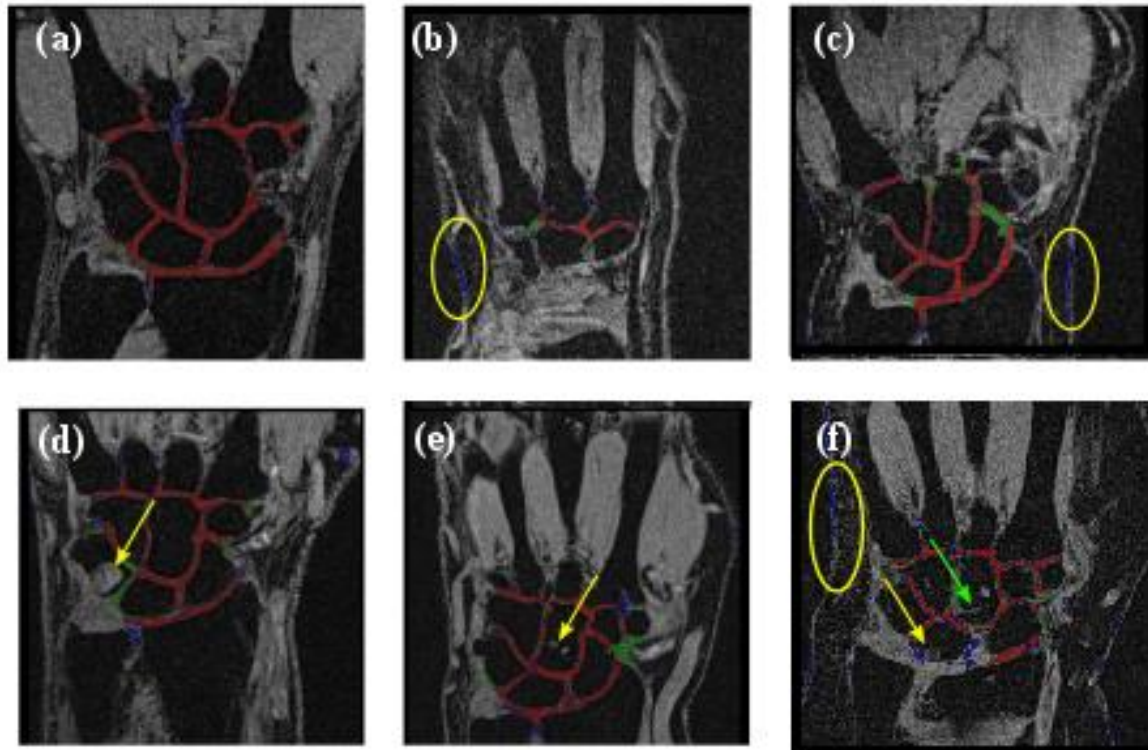


Figure 2. Illustrations of CNN performance: (a) - a medial slice from the validation dataset with good performance (DSC = 0.82); (b) – a lateral slice from the test dataset with medium performance (DSC = 0.72); (c) - a medial slice from the validation dataset with a thin layer of subcutaneous fat considered by CNN as a cartilage; (d, e ,f)- illustrations of CNN performance on the images of unseen patients from the validation dataset. The yellow circles show the subcutaneous fat considered by CNN as a cartilage. The yellow arrows point to the high signal intensity lesions. The green arrow (f) points to the vessel. Red color corresponds to true positives, i.e. pixels correctly segmented as cartilage; green - false negatives, i.e. pixels incorrectly assigned to the background; blue - false positives, i.e. pixels incorrectly assigned to cartilage.

dataset and to segment not only cartilage but other structures such as muscles, bones, ligaments, fat, synovial membrane and liquid as previously described<sup>24</sup>. A 3D approach could also be considered.

The early diagnosis of a cartilage degeneration is essential for a proper choice of treatment modality and leads to a better prognosis of the treatment outcome. Quality of life of patients with OA is usually not very high due to factors such as physical limitations and pain<sup>29,30</sup>. Despite the fact that fewer and fewer people in the modern world are involved in manual labor, the majority of people work with computers, and disability of wrists may have a crucial impact on their working ability. Therefore, wrist joint health preservation remains an important point of the clinical research and new detection methods of early manifestations of OA are needed.

This study was aimed to demonstrate the feasibility of a CNN-based automatic segmentation of wrist cartilage from MR images and was performed in a limited subject data. It can be qualified as Stage 1 from the IDEAL model<sup>31</sup>.

## **CONCLUSIONS**

We have developed a fully automatic method of wrist cartilage segmentation based on a convolutional neural network. The proposed procedure is much faster than the manual one. Moreover, it achieves higher concordance with the ground truth than the several observers. The segmented masks may be used for cartilage volume or cartilage cross-sectional area calculation with the purpose of a quick and comprehensive wrist cartilage quantitative assessment.

## **FUNDING SOURCES**

This work was financially supported by the Government of Russian Federation through the ITMO Fellowship and Professorship Program.

This research was supported by the Ministry of Education and Science of the Russian Federation (Zadanie No. 3.2465.2017/4.6).

This work was financially supported by Government of Russian Federation (Grant 08-08).

This project has received funding from the European Union's Horizon 2020 research and innovation programme under grant agreement No 736937.

## **REFERENCES**

- 1 Eckstein F, Kunz M, Schutzer M, Hudelmaie, M, Jackson RD, Yu J, Eaton CB, Schneider MSE. Two year longitudinal change and test-retest-precision of knee cartilage morphology in a pilot study for the osteoarthritis initiative. *Osteoarthritis Cartilage* 2007;15(11):1326–1332.
- 2 McQueen F, Clarke A, McHaffie A, Reeves Q, Williams M, Robinson E, Dong J, Chand A, Mulders D, Dalbeth N. Assessment of cartilage loss at the wrist in rheumatoid arthritis using a new MRI scoring system. *Ann Rheum Dis* 2010;69:1971-1975.
- 3 Visser AW, Bøyesen P, Haugen IK, Schoones JW, Van der Heijde DM, Rosendaal FR, Kloppenburg M. Radiographic scoring methods in hand osteoarthritis – a systematic literature search and descriptive review. *Osteoarthritis Cartilage* 2014;22(10):1710-1723.
- 4 Link T, Stahl R, Woertler K. Cartilage imaging: Motivation, techniques, current and future significance. *Eur Radiol* 2007;17(5):1135-1146.
- 5 Link T. *Cartilage Imaging: Significance, Techniques, and New Developments*. New York, NY: Springer Science & Business Media; 2011. 93-102 pp.
- 6 Ostergaard M, Bøyesen P, Eshed I, Gandjbakhch F, Lillegraven S, Bird P, Foltz V, Boonen A, Lassere M, Hermann KG, Anandarajah A, Døhn UM, Freeston J, Peterfy ChG, Genant HK, Haavardsholm EA, Mcqueen FAM, Conaghan PhG. Development and Preliminary Validation of

- a Magnetic Resonance Imaging Joint Space Narrowing Score for Use in Rheumatoid Arthritis: Potential Adjunct to the OMERACT RA MRI Scoring System. *J Rheumatol* 2011;38(9):2045-2050.
- 7 Eckstein F, Kunz M, Schutzer M, Hudelmaier M, Jackson RD, Yu J, Eaton CB, Schneider MSE. Magnetic resonance imaging (MRI) of articular cartilage in knee osteoarthritis (OA): morphological assessment. *Osteoarthritis Cartilage* 2006;14:46–75.
- 8 Zink JV, Souteyrand P, Guis S, Chagnaud C, Fur YL, Militianu D, Mattie JP, Rozenbaum M, Rosner I, Guye M, Bernard M, Bendahan D. Standardized quantitative measurements of wrist cartilage in healthy humans using 3T magnetic resonance imaging. *World Journal of Orthopedics* 2015; 6(8): 641-648
- 9 Peterfy CG, Van Dijke CF, Janzen DL, Glüer CC, Namba R, Majumdar S, Lang P, Genant HK. Quantification of articular cartilage in the knee with pulsed saturation transfer subtraction and fat-suppressed MR imaging: optimization and validation. *Radiology* 1994;192(2):485-91.
- 10 Peterfy CG, Van Dijke CF, Lu Y, Connick TJ, Kneeland JB, Tirman, PF, Lang P, Dent S, Genant H.K. Quantification of the volume of articular cartilage in the metacarpophalangeal joints of the hand: accuracy and precision of three-dimensional MR imaging. *AJR Am J Roentgenol* 1995;165(2):371–375.
- 11 Nishimura K, Tanabe T, Kimura M, Harasawa A, Karita K, Matsushita T. Measurement of articular cartilage volumes in the normal knee by magnetic resonance imaging: can cartilage volumes be estimated from physical characteristics? *J Orthop Sci* 2005;10(3):246-252.
- 12 Sittek H, Eckstein F, Gavazzeni A, Milz S, Kiefer B, Schulte E, Reiser M. Assessment of normal patellar cartilage volume and thickness using MRI: an analysis of currently available pulse sequences. *Skeletal Radiol* 1996;25(1):55-62.
- 13 Maataoui A, Graichen H, Abolmaali ND, Khan MF, Gurung J, Straub R, Qian J, Hinterwimmer S, Ackermann H, Vogl TJ. Quantitative cartilage volume measurement using MRI: comparison of different evaluation techniques. *Eur Radiol* 2005;15(8):1550-1554.
- 14 Piplani MA, Disler DG, McCauley TR, Holmes TJ, Cousins JP. Articular cartilage volume in the knee: semiautomated determination from three-dimensional reformations of MR images. *Radiology* 1996;198:855– 859.
- 15 Liukkonen MK, Mononen ME, Tanska P, Sarakkala S, Nieminen MT, Korhonen RK. Application of a semi-automatic cartilage segmentation method for biomechanical modeling of the knee joint. *Comput Methods Biomech Biomed Engin* 2017;20(13):1453-1463.
- 16 Fernquest S, Park D, Marcan M, Palmer A, Voiculescu I, Glyn-Jones S. Segmentation of hip cartilage in compositional magnetic resonance imaging: A fast, accurate, reproducible, and clinically viable semi-automated methodology. *J Orthop Res* 2018;36:2280-2287.

- 17 Folkesson J, Dam EB, Olsen OF, Pettersen PC, Christiansen C. Segmenting Articular Cartilage Automatically Using a Voxel Classification Approach. *IEEE Trans Med Imaging* 2007;26(1):106–115.
- 18 Kashyap S, Oguz I, Zhang H, Sonka M. Automated Segmentation of Knee MRI Using Hierarchical Classifiers and Just Enough Interaction Based Learning: Data from Osteoarthritis Initiative. In: Springer, International Conference on Medical Image Computing and Computer-Assisted Intervention: Springer, 2016;9901:344-351.
- 19 Vincent G, Wolstenholme C, Scott I, Bowes M. Fully automatic segmentation of the knee joint using active appearance models. In: Proceedings of MICCAI Workshop on Medical Image Analysis for the Clinic, 2010;224–230.
- 20 Lee JG, Gumus S, Moon CH, Kwok CK, Bae KT. Fully automated segmentation of cartilage from the MR images of knee using a multi-atlas and local structural analysis method. *Med Phys* 2014;41(9):092303. doi: 10.1118/1.4893533.
- 21 Prason A, Petersen K, Igel C, Lauze F, Dam E, Nielsen M. Deep feature learning for knee cartilage segmentation using a triplanar convolutional neural network. In: *Med Image Comput Comput Assist Interv* 2013;16(Pt 2):246-53.
- 22 Norman B, Pedoia V, Majumdar S. Use of 2D U-Net Convolutional Neural Networks for Automated Cartilage and Meniscus Segmentation of Knee MR Imaging Data to Determine Relaxometry and Morphometry. *Radiology* 2018;288(1):172-185.
- 23 Liu F, Zhou Z, Jang H, Samsonov A, Zhao G, Kijowski R. Deep convolutional neural network and 3D deformable approach for tissue segmentation in musculoskeletal magnetic resonance imaging. *Magn Reson Med* 2018;79:2379-2391.
- 24 Zhou Z, Zhao G, Kijowski R, Liu F. Deep convolutional neural network for segmentation of knee joint anatomy. *Magn Reson Med* 2018;00:1–12.
- 25 Shchelokova AV, Van den Berg CAT, Dobrykh DA, Glybovski SB, Zubkov MA, Brui EA, Dmitriev DS, Kozachenko AV, Efimtcev AY, Sokolov AV, Fokin VA, Melchakova IV, Belov PA. Volumetric wireless coil based on periodically coupled split-loop resonators for clinical wrist imaging. *Magn Reson Med* 2018;00:1–12.
- 26 Dice LR. Measures of the Amount of Ecologic Association Between Species. *Ecology* 1945;26(3):297–302.
- 27 Jaccard P. Distribution de la flore alpine dans le Bassin des Dranses et dans quelques regions voisines. *Bulletin de la Société vaudoise des sciences naturelles* 1901;37(140):241—272.
- 28 Landis JR, Koch GG. The Measurement of Observer Agreement for Categorical Data. *Biometrics* 1977;33( 1):159-174

29 Bodhani, AR, Suryavanshi M, Medema J, Fuldeore M. Health related quality of life among patients with erosive hand osteoarthritis in The United States. *Osteoarthritis Cartilage* 2016;24(Suppl 1)P238.

30 Malm K, Bergman S, Andersson ML, Bremander A, Larsson I, Quality of life in patients with established rheumatoid arthritis: A phenomenographic study. *SAGE Open Medicine* 2017;5:2050312117713647.

31 McCulloch P, Altman DG, Campbell WB, Flum DR, Glasziou P, Marshall JC, Nicholl J, Collaboration B, Aronson JK, Barkun JS, Blazeby JM, Boutron IC, Campbell WB, Clavien PA, Cook JA, Ergina PL, Feldman LS, Flum DR, Maddern GJ, Nicholl J, Reeves BC, Seiler CM, Strasberg SM, Meakins JL, Ashby D, Black N, Bunker J, Burton, M, Campbell M, Chalkidou K, Chalmers I, de Leval M, Deeks J, Ergina PL, Grant A, Gray M, Greenhalgh R, Jenicek M, Kehoe S, Lilford R, Littlejohns P, Loke Y, Madhock R, McPherson K, Meakins J, Rothwell P, Summerskill B, Taggart D, Tekkis P, Thompson M, Treasure T, Trohler U, Vandenbroucke J. No surgical innovation without evaluation: the IDEAL recommendations. *Lancet* 2009;374(9695):1105-1112.

